Send Orders for Reprints to reprints@benthamscience.ae

Current Smart Materials, 2018, *3*, 1-18

REVIEW ARTICLE

Advances in Colloidal Processing of Rare Earth Particles

Silas C. Santos*, Orlando Rodrigues and Leticia L. Campos

Instituto de Pesquisas Energeticas e Nucleares - IPEN, Av. Prof. Lineu Prestes 2242, Cidade Universitaria, Sao Paulo, Brazil

Abstract: ***Background:*** New insights into materials science provide development of smart nano/micro structured materials for advanced applications. Rare earth includes a set of chemical elements (from La to Lu, including Sc and Y) with unique properties, the use of which is evidenced by luminescence applications. Colloidal processing offers great possibilities to obtain smart materials by controlling inter-particle forces, as well as their evolution during ceramic processing. The present article reports a review on colloidal processing with emphasis on rare earth powders. A general view about rare earths properties, including scientific investigations and applications are also presented.

Methods: General view on rare earth sources, classification, properties, studies, and applications are reported. Besides, a review on colloidal processing covering particle characteristics, inter- particle forces, dispersion methods, rheology of suspensions, shaping process, drying-sintering stage, and microstructure formation is reported.

Results: Yttria is the most used rare earth oxide in phosphors applications (70%). Synthesis routes imply on powder properties. Particle characteristics as size, shape, density, and surface area are important parameters for colloidal processing. The control of inter- particle forces by zeta potential evaluation and using dispersion methods provide conditions to prepare stable suspensions. Consolidation of colloidal particles into a desired shape depends on both viscosity and rheological behavior of suspensions. Drying-sintering conditions are effective on microstructure formation and component characteristics. Bio-prototyping is a low cost method, which provides components with complex shape and cellular architecture.

Conclusion: Rare earths exhibit remarkable properties, being applied in diverse technological end-use. Colloidal processing provides opportunities to form smart materials since synthesis of colloids until development of complex ceramic components by shaping methods and thermal treatment. Even though colloidal processing is quite mature, investigations on rare earths involving inter- particle forces, shaping, drying-sintering stage, and microstructure formation are very scarce.

ARTICLE HISTORY

Received: April 11, 2017
Revised: June 07, 2017
Accepted: August 15, 2017

DOI:
10.2174/2405465802666171012143956

Keywords: Colloidal processing, dispersion, particles, rare earths, rheology, shaping, sintering, smart materials.

1. INTRODUCTION

Colloidal processing consists in a set of procedures to obtain advanced materials since manipulation of molecular structures by synthesis, including the control of inter-particle forces (dispersion mechanisms), consolidation of colloidal particles into a desired shape, followed by physical enhancement of particle-particle bonds by means of thermal treatment. Literature [1] defines "colloidal" particles that exhibit diameter size between 1-1000nm.

With advancement in colloidal processing approaches, the use of rare earth elements (RE) in the development of advanced materials has increased considerably. RE is a group of elements that exhibit unique properties, being studied and applied in a diversity of subject areas, from economy to aerospace.

The present paper aims to report a review on colloidal processing of RE based materials. This review is structured as following. A slight overview on RE, including sources, physical-chemical characteristics, searches by subject area, applications, a highlight about yttria, which is the main host material used for luminescent materials, is described.

The behavior of colloidal particles in aqueous medium is a consequence of interaction between particles surface and liquid medium. This interaction is characterized by surface chemistry and determines if particles stay dispersed, flocculated, or become sedimentary. A brief review on surface potential, electric double layer, isoelectric point, and zeta potential definition is reported with the aim to describe the mechanism of dispersion of particles. Besides, the flow behavior of ceramic suspensions, which is defined by how

* Address correspondence to this author at the Instituto de Pesquisas Energeticas e Nucleares - IPEN, Av. Prof. Lineu Prestes 2242, Cidade Universitaria, Sao Paulo, Brazil; Tel: + 55 11 31339670;
E-mail: silas.cardoso@usp.br

2405-4658/18 $58.00+.00

particles interact with each other, including dispersing medium is explained by rheology and rheological models. In addition, optimized parameters from colloidal processing of rare earth based materials are reported.

The control of suspension structure by application of suitable dispersion mechanism provides conditions to form compact bodies with near net shape characteristics. Among shaping methods from suspensions as casting, tape casting, hot pressing, replica is characterized as low cost and effective to produce bodies with complex size, shape, including those with void space. A glance about this useful process is presented.

Finally, an outlook on colloidal processing of RE including chemical, environmental, and biological sciences are described.

2. GENERAL VIEW ON RARE EARTHS

The term rare earths (RE) is given to a group of chemical elements which compose the lanthanide series (from La to Lu), including Sc and Y elements. RE elements are relatively abundant in earth's crystal as shown in Table **1** [2]. Cerium (Ce) is the most abundant among RE with concentration of 60ppm, being higher than copper (Cu) with concentration around 50ppm. Comparatively, lutetium (Lu) is the less abundant among RE with estimative of 0.5ppm. Sc and Pm elements are not indicated in Table **1** since Sc concentration is too small as compared to other RE, as well as Pm is synthetic element [3]. Yttrium (Y) element even though light (atomic number 39), is included with the heavy RE group due to its similar chemical and physical properties [2].

Table 1. Estimative of RE elements available in earth's crust.

Group	Element	Symbol	Atomic Number (Z)	Crust Abundance (ppm)
Light	Lanthanum	La	57	39
	Cerium	Ce	58	66.5
	Praseodymium	Pr	59	9.2
	Neodymium	Nd	60	41.5
	Samarium	Sm	62	7.05
	Europium	Eu	63	2.0
	Gadolinium	Gd	64	6.2
Heavy	Terbium	Tb	65	1.2
	Dysprosium	Dy	66	5.2
	Holmium	Ho	67	1.3
	Erbium	Er	68	3.5
	Thulium	Tm	69	0.52
	Ytterbium	Yb	70	3.2
	Lutetium	Lu	71	0.8
	Yttrium	Y	39	33

In nature, RE elements exhibit aspect like earths, frequently being a mixture of at least two RE elements. Since RE exhibits chemical and physical similarity, the process for separation, which means purification of these elements, is very complex and as a consequence expensive. The first step for separation of RE elements consists in classification of RE elements based on their molecular weight, being separated in light, medium and heavy concentrates. Afterwards, for each concentrate, a process to separate RE elements individually is performed. Thus, the term "rare earths" in fact means "complex to obtain" and consequently, RE based materials are expensive products.

According to the United States Geological Survey (USGS) report of 2017 [4], the main sources of RE are located in China with 36%, Vietnam and Brazil each one with 18%, and Russia with 15% as illustrated in Fig. (**1**). On the other hand, Zhanheng *et al.* [3] reported that Brazil has a large reserve of rare earths around of 32.32%, being bigger than China with 22.12%. However, most of Brazilian reserves might not be practical or economical to process. It is reported that Brazil has begun to process rare earths since 1884.

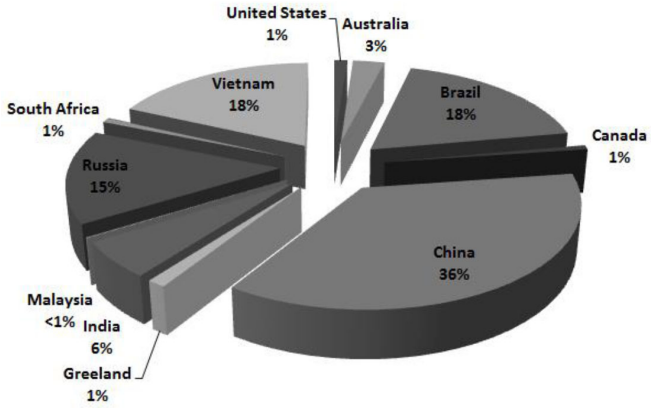

Fig. (1). World RE reserves based on USGS report 2017 [4].

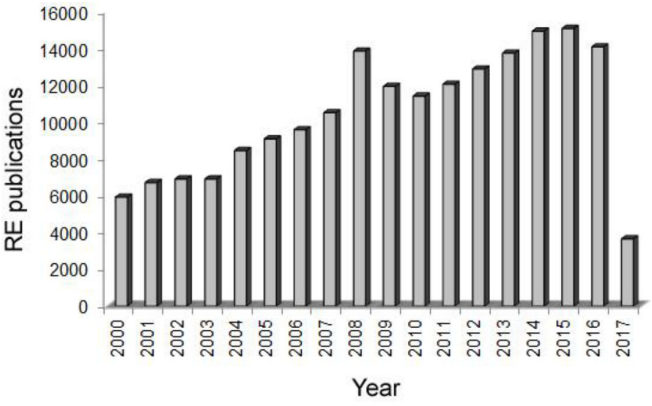

Fig. (2). Scientific contributions on RE based materials from 2000 year up to march 2017 from Scopus platform.

Efforts have been made by the universities and research institutes throughout the world for development of advanced processes to produce materials and components based on RE. Fig. (**2**) Illustrates the scientific search scope on RE based materials in the last seventeen years. The following

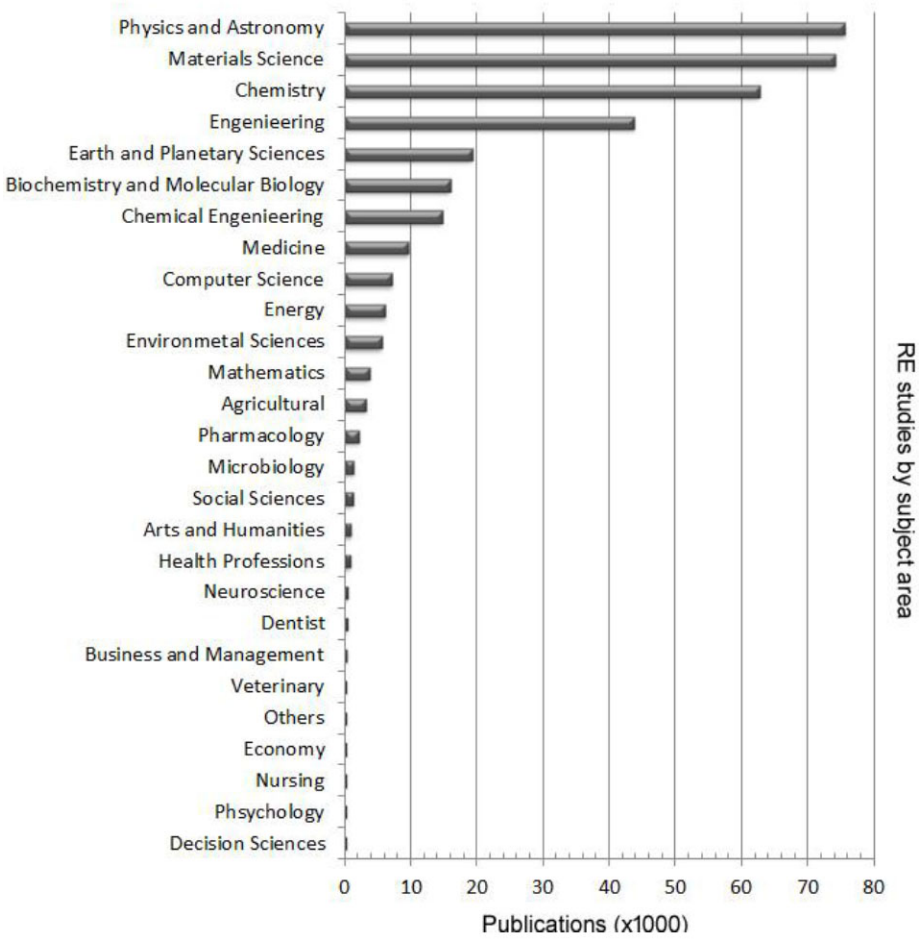

Fig. (3). RE studies by subject area from 2000 year up to march 2017 based on Scopus platform.

keywords were used on Scopus platform in order to build the chart: rare earths, phosphors, lanthanides and, luminescence. Since 2000 year an expressive increase of publications from 6000 to around 15000 in 2015 is observed. A slight difference of less 1000 works is observed in 2016. This difference might be ascribed to difficulties for publishing new papers since peer reviewing process has been improved. For 2017 year only publications up to month of March were considered. However, it is expected that for 2017 a great number of publications like previous years will be reached.

The First Industrial Revolution began with the use of water force and steam as energy supply to improve production. Afterwards, the Second Revolution used electricity in order to perform mass production. With the advance in electronic and information technologies automation of production became reality, which characterized The Third Revolution. A new era of development addressed as Fourth Revolution has begun, characterized as global transformation in which digital, physical, chemical, and biological sciences converge. The RE based materials with their unique physical-chemical properties provide basis for this convergence. The result of this convergence is illustrated in Fig. (**3**) that relates the main searches using RE by subject area. The ten top search areas according to the number of publications are as following, (1) Physics and Astronomy, (2) Materials Science, (3) Chemistry, Engineering, (4) Earth and Planetary Sciences, (5) Biochemistry and Molecular Science, (6) Chemical Engineering, (7) Medicine, (8) Computer Science, (9) Energy, and (10) Environmental Sciences.

Innovation is a drive force that provides development and this concept is represented on RE end-use and investigation (Fig. **4**). The three biggest economies concentrate the most efforts on new insights on RE based technology as follows, China (29.14%), United States (14.54%) and Japan (9.09%). Despite China, the BRICs group presents significant participation on RE studies around 13.61%. Considering recent release of The Global Competitiveness Report 2016-2017 [5], technology and innovation are increasingly driving development. In addition, developing economies like BRICs exhibit large market size which is attractive for application of new policies and strategies of development.

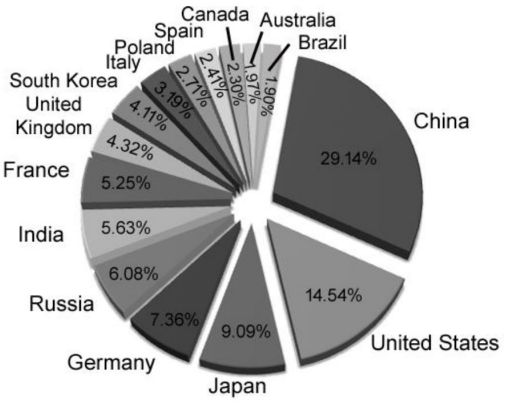

Fig. (4). Top 15 countries that concentrate effort on RE based studies from 2000 year up to march 2017 according to Scopus platform.

RE elements present chemical and physical similarity, exhibiting quite similar structure of external electronic levels 5d and 6s. The sublevel 4f is progressively filled and ionic and atomic radius decrease as a function of atomic number (Z). This peculiarity is characterized as lanthanide contraction and reflects in properties of RE atoms and ions as, enhancement of complexes formation stability, less tendency of metals oxidation, hydrolysis and, improvement of covalence degree [6].

The use of RE based materials (Fig. **5a**) has increased significantly in diverse technological applications and searches on this field have provided many advances in magnets [7], special alloys [8], glass pigments [9], optical fibers [10], lenses [11], abrasives [12], thin films [13], sintering aids [14], luminescence materials [15], oxygen sensors [16], cracking catalyzers [17], cancer treatment [18] and odontology [19].

Ce and La based oxides are the most used with respectively 43.5**%** and 39.9**%** as illustrated in Fig. (**5b**). According to the recent report of USGS [20], La_2O_3 is used for the production of digital camera lenses, including cell phone cameras (>50%), including catalyzers to refine petroleum. Ce based oxide is used in automotive catalytic converters, as well as making special alloys.

Nowadays, among RE group yttrium oxide also known as yttria (Y_2O_3) is one of the most important oxides, being used in a variety of applications. In this work this substance will be addressed as yttria and a special glance on this material is given as following.

3. YTTRIA (Y_2O_3)

Yttria exhibits cubic C-type crystal structure (Fig. **6a**), density of 5.02g.cm^{-3}, melting point at 2400°C, and other intrinsic properties (Table **2**) [21] that gives rise to it as a promising material for advanced applications. Hoekstra *et al.* [22] reported that all sesquioxides as Dy_2O_3, Th_2O_3, Ga_2O_3 and Ln_2O_3 present C-type structure. Nevertheless, some contributions in literature revealed Y_2O_3 exhibiting other three distinct crystal structures. Gourlaouen *et al.* [23] synthesized Y_2O_3 with monoclinic structure at 997°C using pressure of 2GPa. Navrotsky *et al.* [24] reported that cubic C-type structure exhibited two phase transformations, the first from cubic to fluorite at 2308°C and, the second from monoclinic to hexagonal at 2325°C. Quin *et al.* [25] observed that yttria particles with diameter less than 10nm exhibited monoclinic structure.

As crystallographic characteristic of Y_2O_3, the cubic C-type lattice is composed of Ia3 space group, sixteen formula units per unit cell, coordination number (N) of 6, and two points symmetry (S_6, C_{3i}) and C_2. The S_6 site has an inversion center and smaller crystal field, whereas C_2 has no center of inversion, which enables electron-dipole transitions and consequently luminescent emissions as doped with RE ions. Doping yttria host with RE is performed by replacing Y^{3+} ions with Eu^{3+} at sites S_6 and C_2. A small cluster model containing four Y and six O atoms from Y_2O_3

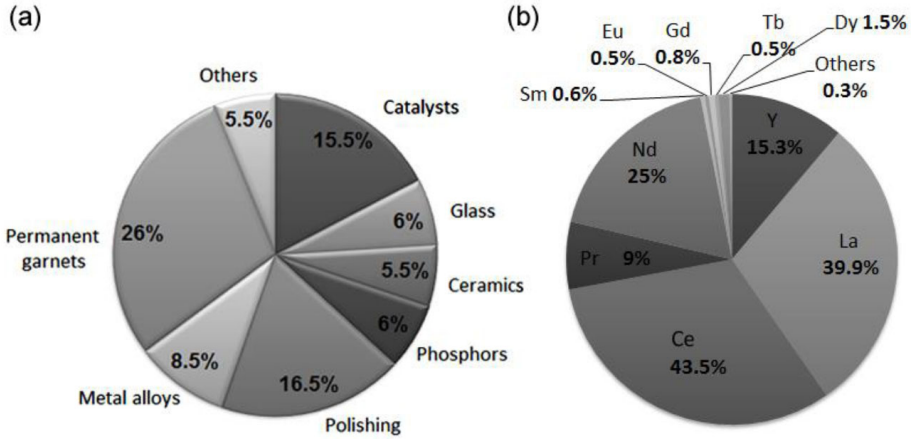

Fig. (5). Applications of RE based materials in the world by (**a**) subject area, (**b**) oxides.

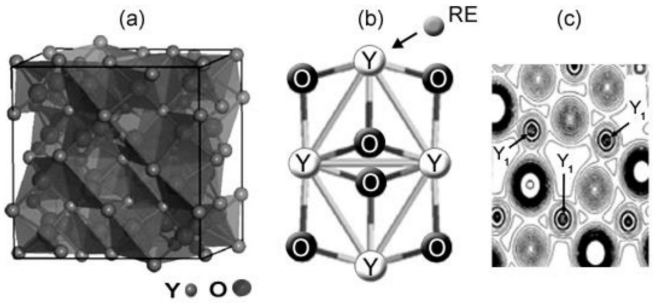

Fig. (6). Crystallographic representation of yttria. In (**a**) Cubic C-type crystal structure, (**b**) C_2 cluster (**c**) valence charge density map.

Table 2. Main properties of yttria.

Properties	Description		
Physical	Density (g.cm^{-3})		5.02
	Refractive index		>1.9
	Melting point (°C)		2400.0
	Crystalline structure		Cubic C-type
	Band gap (eV)		5.6
	Phonon energy (cm^{-1})		300-380.0
Mechanical	Vickers hardness (GPa)		6.0
	Flexural Strength (MPa)		130.0
	Young's modulus of elasticity (GPa)		160.0
	Fracture toughness (MPa.m$^{1/2}$)		1.1
Thermal	Coefficient of linear thermal expansion (x10^{-6}.K^{-1})	40-400°C	7.2
		40-800°C	7.6
	Thermal conductivity (W.m^{-1}.K^{-1})	20°C	14.0
	Specific heat capacity (J.g^{-1}.K^{-1})	0.45	
Electrical	Dielectric strength (kV.mm^{-1})	11.0	
	Volume resistivity (Ω.cm)	20°C	>10^{13}
		300°C	10^{10}
		500°C	10^{7}
	Dielectric constant	1MHz	11.0
	Dielectric loss angle (x10^{-4})	1MHz	5.0
	Loss factor (x10^{-4})	55.0	

lattice (C_2 symmetry) is illustrated in Fig. (**6b**). Govindasamy *et al.* [26] using the time-dependent density functional theory (DFT) calculated binding energies of undoped and Eu doped yttria. As a result, authors found out that most probable transition in yttria cluster is a singlet state with binding energy around -58.46eV.

Some investigations reveal that the nature of bonding between Y-O is not completely ionic. Nian Xu *et al.* [27] reported a theoretical study on the bond order of Y_2O_3, which means a quantitative measure of the strength of the bond for Y and O in crystal lattice of Y_2O_3. From this study, the chemical bond of Y_2O_3 is far from fully ionic and the bonding between Y and O is significantly covalent. In addition, from the valence charge density maps (Fig. **6c**) [27] it is seen that the cubic structure of Y_2O_3 is less closely packed, exhibiting large vacancies for Y and O planes. As a result, these vacancies enable RE ions incorporation and formulation of luminescent yttrium oxide based materials (Y_2O_3:RE).

Yttria exhibits chemical and physical properties quite similar to lanthanides elements, being very used as matrix for insertion of other RE ions (activators) and forming luminescence materials. The emission spectrum varies as a function of RE ion as well as its concentration. Wang *et al.* [28] reported that europium doped yttria (Y_2O_3:Eu) emission was intensified according to the crystallite and particle size of particles. Besides, Zhang *et al.* [29] observed significant luminescence of Y_2O_3:Eu as synthesized by combustion method and sintering in vacuum atmosphere. In addition, Goldburt *et al.* [30] particles with size around 1nm exhibited higher emission than those with size around 10nm. Face to this context, it is seen that yttria is a very useful substance for the composition of luminescence materials.

As shown in Fig. (**7a**), yttria is basically used for ceramic (47%) and phosphors (43%) development. For ceramics, yttria is used as structure aid for advanced ceramics as ZrO_2 (TZP) [31], aluminium and magnesium based alloys [32], biomaterials [33], and permanent magnets [34].

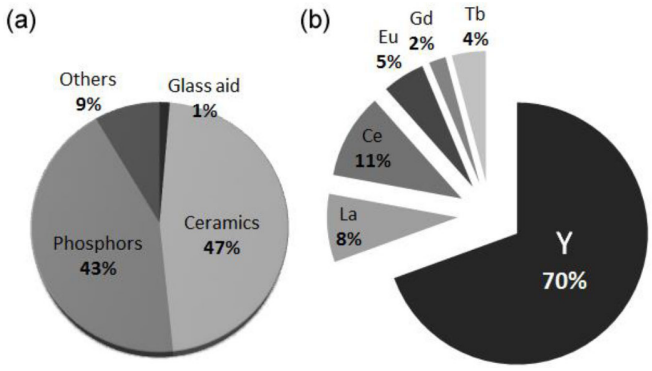

Fig. (7). Yttrium oxide as high technological material, (**a**) general use and (**b**) as host for phosphors technology.

For phosphors application (Fig. **7b**), yttria is the most used material as compared with others RE (70%), being used mostly as host for other RE such as Y_2O_3:Er [35]; Y_2O_3:(Er, Tb) [36]; Y_2O_3:Eu [37]; Y_2O_3 (Eu, Dy, Tb) [38]. Besides, yttria-alumina system provides an excellent material for laser technology as YAG (yttrium aluminium garnet) [39]. Therefore, yttria exhibits large applicability and its use as controlled provides substantial condition for the development of high advanced materials. Colloidal processing aims at this issue.

Colloidal processing is one of the approaches frequently used to produce ceramic bodies from ceramic suspensions constituting particles which have a diameter size of up to 1000nm. Since particle size is small, the contact area

between particles and dispersing medium is large. As a consequence, surface forces are strongly effective on suspension behavior. The ability of controlling particle stability has led to the advances beyond ceramic processing as, petroleum, filtration systems, inks, drug delivery; cosmetics, and food processing.

4. GENERAL ASPECTS OF COLLOIDAL PROCESSING

Colloidal processing supplies great possibilities to obtain smart materials by means of manipulation of molecular structures (colloids), control of inter-particle forces, consolidation of colloidal particles into a desired shape, drying, and the enhancement of inter- particle bonds by thermal treatment. Our research group has contributed with publications covering this issue as follows, yttria nettings [40]; bio-prototyping of rare earth doped yttria ceramics [41], yttrium disilicate microcellular ceramics [42] and, biomorphic dysprosium doped yttrium disilicate burners [43].

Particle characteristics as size, shape, surface area, density, as well as chemical composition must be well controlled in order to produce smart materials. Diverse synthesis methods have been proposed for production of rare earth particles with controlled characteristics such as sol process [44], micelles [45], sol-gel [46], chemical precipitation [47], hydrothermal [48], pyrolysis [49], and vapour deposition [50]. According to the synthesis method particles can exhibit one of the following shapes, spherical, rounded, angular, spongy, flakey, cylindrical, acicular, and cubic (Fig. **8**).

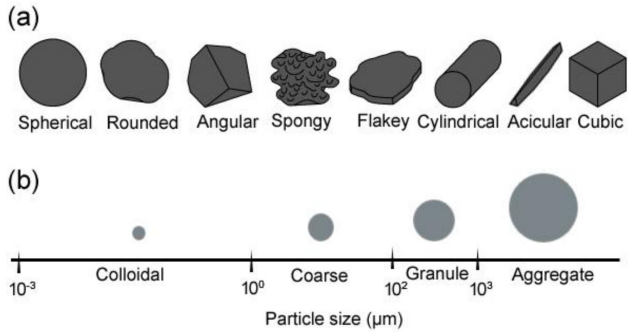

Fig. (8). Classification of particles considering (**a**) size and (**b**) shape.

Particle size is an important parameter in colloidal processing. In general, powder is composed of particles of diverse sizes. Thus, it is fundamental to measure not only the mean particle size (d_{50}), but its size distribution. Particle size represents the three dimensional particle in one-dimensional scalar value. A good review on techniques for particle size measurements is found in [51].

Particle size distribution, shape, and state of agglomeration have substantial influence on rheology, shaping, drying, and sintering. As a result, the final microstructure which determines material performance is associated with characteristics of starting powders.

A ceramic suspension consists basically in a homogeneous mixture of solid particles dispersed in liquid medium. The properties of this mixture (solid particles and liquid medium) depend on characteristics of liquid and particles (size, shape, particle surface condition) and the interface between particle-liquid medium [52].

Stable suspensions supply suitable packing of particles during shaping and as a consequence, leads to the formation of ceramic bodies with high density as shaped, high dimensional control, low concentration of defects, as well as homogeneous microstructure as sintered [53].

The particle behaviour in suspension and its stability can be understood using Double layer model or DLVO theory (Derjaguin, Landau, Verwey and, Overbeek) [54]. From this model, aqueous suspension stability can be controlled by adjusting surface condition of particles *via* pH of suspension.

Electric potential formed at particle surface (Fig. **9a**) [55] attracts many ions in suspension with opposite charges (contra ions), which in turn stay around particle. Since particle exhibits limited size, only some ions are absorbed on the particle surface. The absorbed contra ions form a protective layer, Stern layer. Those ions that are not absorbed are not able to stay beside particle, seeing that are repealed by Stern layer ions. Contra ions concentration decreases as a function of their distance from solid particle, which in turn forms a second layer addressed as diffuse layer. On the other hand, ions that exhibit charge equal to particle are known as co-ions and are attracted by contra ions from Stern layer and at the same time are strongly repealed by particle. As a consequence, co-ions concentration is intensified by increasing of the distance from particle surface (Fig. **9b**). The region that englobes Stern layer and diffuse layer is defined as double electric layer. This ionic cloud follows particle throughout suspension flow, keeping it dispersed in liquid medium [56].

Based on the Stern theory (Fig. **9c**) [55] the electric potential varies from particle surface (ψ) to Stern plane (ψ_d) and decreases to 0 as a function of distance from particle surface. Electric potential of Stern plane is measured by experimental techniques as electrophorese. By electrophorese an electric field is applied on suspension and the velocity of dislocation of particles (electrophoretic velocity) is measured. From this values and using Equation **1**, it is possible to determine zeta potential (ζ) that represents electric potential at share plane. The share plane includes an area of separation between those remaining contra-ions of double electric layer and those that are not on particle surface as soon as an electric field is applied [56, 57].

$$\zeta = \frac{6\pi\eta\mu_e}{\varepsilon f(k\alpha)} \text{ [mV]} \quad \textbf{(1)}$$

Table 3. IEP of rare earth oxides reported in literature.

Ref.	RE oxide	IEP	Electrolyte	T. (°C)	Equipment
[58]	CeO_2	6-8	10^{-3}M $NaNO_3$	24°C	Pen Kem 501
[59]	Dy_2O_3	8.8	-	-	Pen Kem 7000
[59]	Er_2O_3	8.8	-	-	Pen Kem 7000
[60]	La_2O_3	10.3	-	-	-
[59]	Nd_2O_3	8.4	-	-	Pen Kem 7000
[61]	PrO_2	8.0	10^{-2}M KCl	-	-
[62]	Sc_2O_3	7.2	10^{-2}M KCl	25°C	Rank Mark II
[59]	Sm_2O_3	8.3	-	-	Pen Kem 7000
[63]	Th_2O_3	5.9-7.3	10^{-3} KNO_3/$NaClO_4$	23°C	-
[64]	Y_2O_3	8-9	10^{-2} NaCl	26-27°C	Malvern Zetasizer II C
[61]	Yb_2O_3	6.8-7.2	10^{-2} - 1M NaCl/ KNO_3	25°C	-

Ref.: Reference; T.: Temperature; (-) unavailable data.

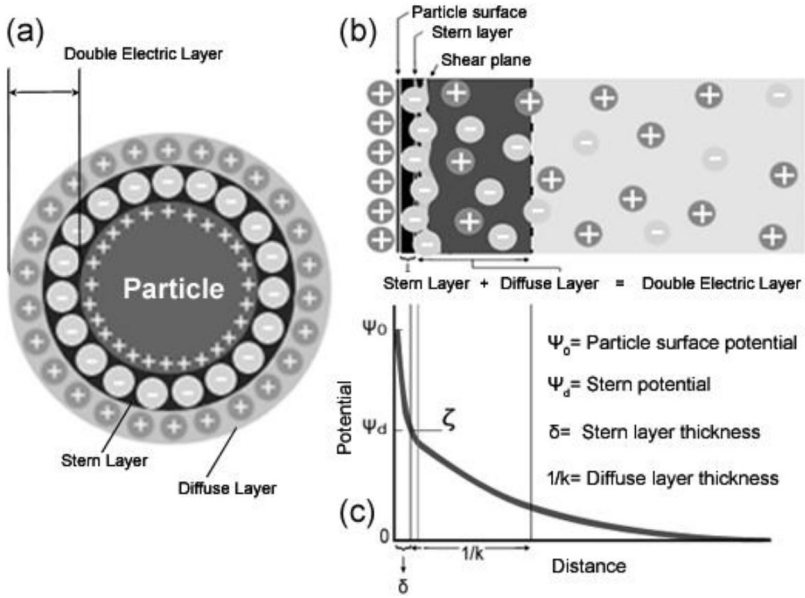

Fig. (9). Representation of the electric double layer according to Stern's theory. In (**a**) particle dispersed in liquid medium surround by ions forming Stern layer, diffuse layer and electric double layer; (**b**) disposition of charge layers that form electric double layer; and (**c**) electric potential variation as a function of the distance from particle surface [55].

Onde:

- ε = electric permissively;
- η = viscosity of medium [mPa.s];
- μ_e = electrophoretic mobility [$\mu.s^{-1}.V^{-1}.cm$];
- $f(k\alpha)$ = 1.5 (aqueous medium).

According to the DLVO theory [54], the stability of particles in aqueous medium is performed by means of pH shifting, which means ionic strength of medium. It is considered that a suspension is stable when zeta potential |Z| value is at least 25mV. If |Z| is zero particles become neutral, wherein no electric double layer is formed. As a consequence, particles tend to be agglomerate and sink. The pH value in which this phenomenon takes place is defined as isoelectric point (IEP). Therefore, to prepare stable suspensions ($|\zeta| \geq 25$mV) it is recommended that pH is shifted for values far from IEP. Table **3** lists the IEP of some RE oxides.

The principle of stability of ceramic suspensions consists in reducing the intensity of attraction forces between particles, as well as increasing the dispersing time of particles. For this purpose procedures are done in order to give rise to repulsion forces and as a consequence maintain particles dispersed. This repulsion methods can be performed by means of electrostatic charges (electric mechanism), repulsion by polymeric molecules (steric mechanism or

depletion), and by combining methods of electric charges with polymeric molecules (electrosteric mechanism).

4.1. Methods of Suspensions Stabilization

Electrostatic stabilization (Fig. **10a**) [65] includes formation of electric charges in particle surface. For oxides, the formation of surface charges usually occur as a result of reaction between (OH^-) surface group and hydroxonium (H_3O^+) and hydroxyl (OH^-) ions of liquid medium, as expressed in Equation **2** [55] and Equation **3** [55]. This process depends on pH of suspension. The development of negative surface charges is enhanced as pH at least equal or superior of 7, whereas for pH less than 7 positive charges are formed. Thus, the origin of surface charges is a consequence of electric potential difference. To disperse particles in a liquid medium the repulsion forces have to overcome attraction forces.

$$MOH + H^+ = MOH_2^+ \quad \textbf{(2)}$$

$$MOH + OH^- = MO^- + H_2O \quad \textbf{(3)}$$

Where,

- H+: ion of positive electric potential (+);
- OH^-: ion of negative electric potential (-);

In some ceramic systems elaboration of stable suspensions only with pH adjustment is not possible, once great concentration of acid or base solutions gives rise to dissolution of solid particles, or increase of ionic strength. As a consequence, electric double layer is shrunk, particles flocculate and finally, sink as sediment. Thus, polymeric dispersants are used to supply stability of particles by a physical barrier from adsorption of polymeric chains in particle surface [56].

Steric stabilization (Fig. **10b**) [65] includes using a polymer as a physical barrier to separate particles in suspension. For this stabilization to be effective, the polymer has to be adsorbed in particle surface so that the bond polymer-surface is intense, avoiding the phenomenon of desorption. The thickness of adsorbed polymeric layer has to be higher than the distance in which Van Der Waals forces act. However, polymer chains cannot be long enough to give rise to phenomenon of bridge, wherein the same polymeric chain is adsorbed by two particles bridging [56].

The interaction between polymer layers adsorbed in particles surface is under the influence of the distance between them. As the distance (D) is double than its thickness (L) of polymeric layer (D>2L), there is no repulsion between particles by this mechanism. If this distance is (L<D<2L) polymer chains can penetrate each other to eliminate the liquid which separates each other (osmotic pressure). When the distance between particles is (D<L) there is a compression of polymer chains while collision of particles, giving rise to a strong repulsion between them.

Electrosteric mechanism is a result of the last two dispersing mechanisms, which are electrostatic and steric. Electrosteric dispersion is based on ionized polymer chains, which are defined as polyelectrolytes. As resulted ions from dissociation of molecules supply dispersion of particles by steric and electrostatic mechanisms (Fig. **10c**) [65].

Particle stabilization can be also performed by means of adding polymer solutions which are not adsorbed in particle surface, and being still in solution. This mechanism is addressed as depletion (Fig. **6d**) and according to Azakura *et al.* [66] as particles tend to be near each other, the polymer which is in the region between them, goes out and leads to flocculation of these particles.

Vicent *et al.* [67] proposed an alternative depletion approach. This model is based on a mixture of steric stabilization and traditional depletion, in which the adsorbed polymer in particle surface (L) interacts with those polymer molecules in dissolution. These free polymer molecules collide with adsorbed polymer. However, as particles are near each other, the free molecules are excluded from the region between particles (D). It is considered as a weak repulsion mechanism. From this model, as the distance (D) of separation of particles is 2L depletion attraction takes place, whereas when the D is less than 2L, steric repulsion is effective.

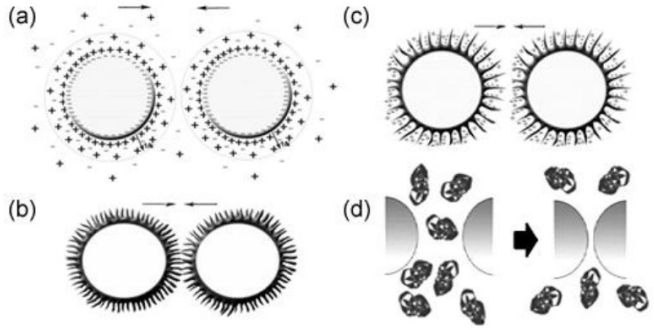

Fig. (10). Methods for dispersing particles in liquid medium, (**a**) electrostatic; (**b**) steric; (**c**) electrosteric; and (**d**) depletion.

Santos *et al.* [40] reported the stability of yttria in aqueous medium using 10^{-2}M NaOH as electrolyte (Fig. **10**) [40]. In this study, zeta potential evaluation of yttria was performed as a function of dispersant concentration (poly-acrylic acid, PAA) and pH from 5.5 to 12.5 (Fig. **10a**) [40]. Sprycha *et al.* [68] reported that yttria particles are soluble in acid conditions, with pH less than 5.5. As a result, it is observed that yttria suspensions with no dispersant (0 wt.% PAA) exhibited an isoelectric point (IEP) at pH of 8.5. Further, yttria particles became stable at pH values inferior of 7 with zeta potential |of 50mV, as well as with pH higher than 9.0 with |ζ| at least of 40 mV.

The use of PAA provided displacement of IEP from 8.5 to around of pH 6-6.5 (Fig. **11a**) [40]. Besides, PAA was useful to prepare stable suspensions apart from pH of 6.5. In

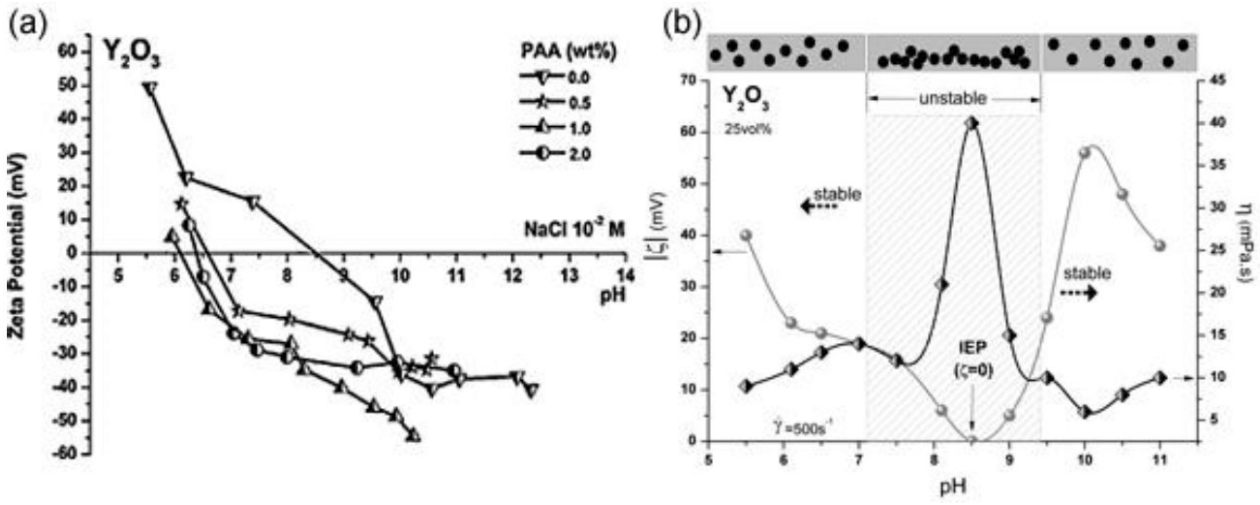

Fig. (11). Evaluation of yttria particles stability in aqueous medium. In (**a**) zeta potential curves as a function of pH and dispersant dosage PAA; (**b**) correlation between zeta potential and viscosity based on pH of suspension.

addition, concentration of 1 wt.% of PAA with pH of 10.5 supplied the highest zeta potential (|56 mV|), being the best parameters to prepare highly stable suspensions.

The effect of zeta potential (ζ) on promoting decrease viscosity (η) of yttria suspensions is shown in Fig. (**11b**) [40]. If pH of suspension is set near to IEP (pH of 8.5) weak dispersion of particles with low zeta potential around of |5 mV|), and as a consequence high viscosity are provided. On the other hand, as long as pH is set to alkaline condition such as pH of 10.5 ζ value became maximum (|40 mV|), whereas η became minimum (7 mPas). Therefore, these results confirm that the pH around 10.5 provides highly stable yttria suspensions.

The stabilization of particle provides preparation of ceramic suspension for any kind of shaping process such as, casting, prototyping, replica, extrusion, injection, dip coating, and tape casting. Based on this idea, rheological behaviour is one of the most important properties in ceramic processing from suspensions. In general, rheology characterizes flow behavior of fluids, suspensions of particles, and emulsions as a response to external stress. Parameters as viscosity, temperature, shear rate, and shear stress are essential variables for materials processing from suspensions.

4.2. Rheology of Ceramic Suspensions

Rheology is the science that studies the relation between deformation and flow of matter [56]. IUPAC [69] describes it as the study of deformation and flow of matter by influence of external tension. This word, which is from Greek and whose composition means rheo > flow and logy > study was proposed for the first time by Bingham in 1928. Rheology aims to determine the necessary force to provide some deformation of matter, which means deformation or flow as resulted of external tension.

In rheological study the important parameters are viscosity, shear rate, shear stress, solids load, and liquid medium (aqueous or organic). The shifting of these parameters is necessary according to the specific conditions for each shaping process [70].

4.3. Viscosity

For diluted suspensions (low solids load), or "pure" substances like water, the viscosity is a constant of proportionality between external tension and velocity of flow (shear rate). Upon concentrated suspensions, this relation is not effective, which means that viscosity involves other parameters [56, 71].

Viscosity constitutes the main rheological characteristic of a suspension. Stable suspensions tend to flow easily as compared with those unstable. As much as particles are in suspension, more complex dispersion is, since the distance between particles become shorter, which makes easier to give rise to attraction forces as Van Der Waals and formation of agglomeration of particles. The agglomerates exhibits void spaces which retain liquid in their interior and intensify friction between particles and as a consequence, enhance viscosity of suspension [56].

4.4. Shear Stress (τ) and Shear Rate ($\dot{\gamma}$)

Among many definitions about viscosity, one which is much appreciable refers to viscosity as the resistance of flowing. Based on the Newton model [65] two parallel plates are separated by a distance (x) and a liquid is between them. The inferior plate (base) is fixed. A force (F) is applicable upon superior plate with area (A) in tangential direction, wherein a plate moves with a constant velocity (V) in parallel direction to inferior plate. The liquid molecules which are beside superior plate will move with velocity (V), which decreases gradually as a function of the

distance of liquid molecules from superior plate, tending to zero for those near inferior plate (base) [71].

The tangential force (F) that acts for the unity of area (A) is defined as shear stress (τ), the force necessary to provide flowing of a fluid and is expressed as shown in Equation **4** [71].

$$\tau = \frac{F_{[N]}}{A_{[m^2]}} \text{ [Pa]} \quad \textbf{(4)}$$

The gradient of velocity of plates defines the shear stress ($\dot{\gamma}$), which is expressed as shown in Equation **5** [71].

$$\dot{\gamma} = \frac{dV}{dx}[s^{-1}] \quad \textbf{(5)}$$

With these two parameters defined (τ) and ($\dot{\gamma}$) viscosity of diluted suspensions like water can be determined, as expressed in Equation **8** [71]. For more complex suspensions, other parameters are considered in order to calculate viscosity, wherein additional mathematical models are used.

$$\eta = \frac{\tau}{\dot{\gamma}} \text{ [Pa.s]} \quad \textbf{(8)}$$

The viscosity of suspensions can be affected by parameters as chemical composition, temperature, pressing, shear rate, and electric and magnetic field. Among these parameters, the most important based on rheological view is the shear rate ($\dot{\gamma}$). The graphical representation of shear stress (τ) x shear rate ($\dot{\gamma}$) is a flow curve [71].

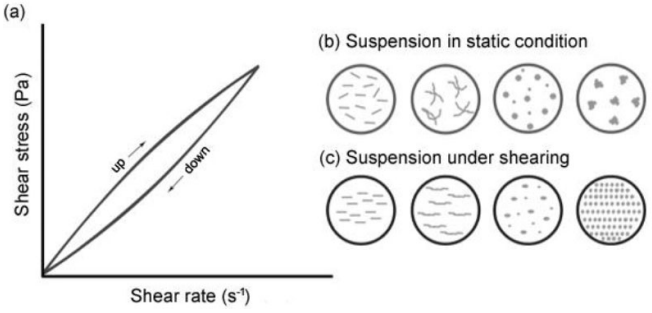

Fig. (12). Rheology of ceramic suspensions. In (**a**) flow curve composed by up and down curves; structure of suspensions while (**b**) static and (**c**) under shearing [72].

4.5. Flow Curves

The flow curves are used in the studies of viscosity when a fluid or suspension of solid particles is flowing. In this concept, the flow behavior of suspension can be determinated by variation of shear stress (τ), or shear rate ($\dot{\gamma}$). In general, the flow plots (Fig. **12**) [72] are composed of two curves, one addressed as up and other as down, which correspond to rising and downing of shear rate ($\dot{\gamma}$) as function of time. Based on the flow curves, the rheological behavior can be classified as Newtonian, Bingham, dilatant, and shear thinning [71].

4.6. Rheological Models

Newtonian fluids exhibit viscosity independent of shear rate, which means the viscosity, is a proportional constant between share rate and shear stress (Fig. **12**). This kind of behavior is characteristic of "pure" fluids like water and highly diluted suspensions such as mineral oil and bitumen [56, 71].

Shear thinning behavior includes decrease in viscosity as a function of shear stress. Some materials that exhibit this behavior are: shampoo, inks, and syrup. Some parameters that can provide shear thinning behavior are break down of agglomerates of particles, orientation and deformation of particles, stretching of long polymer chains. If the decrease in viscosity depends on time, the fluid is characterized as thixotropic [56, 71].

Dilatant behaviour means that viscosity increases as a function of shear rate increase. Most suspensions do not exhibit shear thickening flow, but shear thickening can give rise to highly stable concentrated suspensions, as well as with those based on dispersed particles in medium wherein aids are used. In this case, particles are separated by thin liquid film. To provide displacement of particles through suspension a liquid between particles is necessary and this gives rise to only low shear rate. For high shear rate, the thin liquid layer is not enough to lubricate particle surface and as a consequence viscosity increases. For suspensions with plasticizers this aid fills all voids between particles and lubricates their surface. During sharing, suspension behavior is analogue with those described previously. If the increase of viscosity depends on time, the fluid is characterized as rheopectic [56, 71].

Bingham fluids include systems in which flow behavior depends on an external force which presents a minimum tension to provide flowing. Apart from this, the fluid can present one or more rheological behaviours (Fig. **13**) [56, 71].

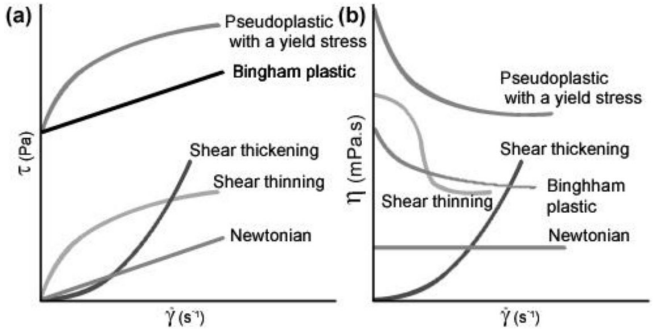

Fig. (13). Representation of rheological behavior of fluids. In (**a**) flow curves and (**b**) viscosity curves.

Table 4. Main rheological models.

Modelo	Equação
Newton	$\tau = \eta\dot{\gamma}$
Bingham	$\tau = \tau_0 + \eta_p\dot{\gamma}$
Ostwald - de - Waele	$\tau = k(\dot{\gamma})^n$
Herschel-Bulkley	$\tau = \tau_0 + k(\dot{\gamma})^n$
Casson	$\tau^{1/2} = (\tau_0)^{1/2} + k_1(\dot{\gamma})^{1/2}$
Casson modificado	$\tau^{1/2} = (\tau_0)^{1/2} + k_1(\dot{\gamma})^{n_1}$
Ellis	$\dot{\gamma} = k_1\tau + k_2(\tau)^{n_1}$
Herschel-Bulkley modificado	$\tau^{n_1} = (\tau_0)^{n_1} + k_1(\dot{\gamma})^{n_2}$
Séries de Potência	$\tau = k_1\tau + k_2\tau^3 + k_3\tau^5 \ldots$
Cross	$\frac{\eta_0 - \eta}{\eta - \eta_\infty} = (k\dot{\gamma})^m$
Carreau	$\frac{\eta - \eta_\infty}{\eta_0 - \eta_\infty} = \frac{1}{[1 + (k_1\dot{\gamma})^2]^{m_{1/2}}}$

K_1, K_2, K_3, n_1 e n_2 are arbitrary constants and power index which are determined by experimental data.

Suspensions used in industry can exhibit one or more rheological behaviours as a function of shear stress applied, processing and materials condition. Based on this concept, mathematical models (Table **4**) were proposed in order to describe rheological behaviours of suspensions by mathematical fit.

Colloidal processing aims to consolidate suspensions in green bodies with homogeneous shape and dimensions. The as shaped body must exhibit minimum mechanical strength in order to be handled without shape deformation or cracking. Several shaping methods have been developed to produce ceramic components of varying shape, size, and microstructure. For this purpose, the rheological characteristics of suspensions must be controlled for each shaping method.

4.7. Fitting the Structure of Ceramic Suspension for Shaping

The way how particles are in suspension, which means the condition of dispersion (high, medium, low), affect directly the viscosity of suspension, and as a consequence its flow behavior. Therefore, the requirements for stabilization of a ceramic suspension depend on the shaping process chosen.

Even though many effective synthesis methods have been proposed for the production of rare earth materials, there are few studies about stabilization of RE particles in suspension. Studies about rheology of rare earth systems studies are quite rare. The lack of investigations concerting rheology of RE might be due to the rheological evaluation. To perform a rheology study is necessary a substantial quantity of material to prepare suspensions (samples). Besides, RE are still high cost materials, which in economic terms complex their use in great quantity.

Many process are used to shape ceramic materials from suspensions with low, medium and high solids load such as, slip casting [73], tape casting [74], pressure filtration [75], osmotic consolidation [76], three-dimensional printing [77], centrifugal consolidation [78], aqueous injection molding [79], gel-casting [80], direct coagulation casting [81], extrusion [82], electrophoretic deposition [83], replica [84], dip coating [85], and spray drying [86]. Each of these processes is under different tension and for each situation suspensions have to exhibit specific characteristics, which are dependent on materials characteristics as, size and shape of particles, dispersing, density, and temperature. According to this idea these are specific parameters for each shaping process: stability and rheology of ceramic suspensions, temperature, drying, shape and dimensions of the as shaped material. Table **5** summarizes the shaping methods from colloidal suspensions.

Table 5. Summary consolidation of particles by shaping methods.

Shaping Method	Description
Slip casting	Suspension flows into porous template driven by capillary forces
Tape casting	Suspension flows through a doctor blade on a flat surface.
Pressure filtration	Suspension flows through a porous filter driven by an applied pressure
Osmotic consolidation	Suspension flows through a semipermeable membrane driven by osmotic pressure difference
3D printing	Colloidal gel is formed as a result of flocculation of particles
Centrifugal consolidation	Suspension flows due to applied gravitational force
Aqueous injection molding	Colloidal gel is formed as a function of temperature change
Gelcasting	Chemical reaction leads to formation of a cross-linked organic network
Direct coagulation casting	Colloidal gel is formed by flocculation of particles
Extrusion	Suspension flows through a shaped opening in a die by a ram pressure.
Electrophoretic deposition	Particles flow as a result of applied electric field
Replica	Suspension flows through a reticulated template by immersion
Dip coating	Suspension flows driven by substrate immersion speed as well as its withdrawing
Spray drying	Suspension flows like droplets driven by pump

Table **6** lists some approaches on colloidal processing of rare earth based materials, in which essential parameters for rheology of suspensions as solids load (particles), pH of medium, dispersant dosage, and binder are presented.

Table 6. Processing parameters used to prepare stable RE suspensions by shaping process.

Process	Suspension	Vol.%	pH	Dispersant (wt.%)	Binder (wt.%)	Ref.
Replica	$Y_2Si_2O_7$:Dy	25%	10.0	2.0%PAA	0.4%CMC	[43]
	CeO_2:Ga	40%	7.0	5.0%PVA	5.0%PEG	[79]
	RE_2O_3	25%	10.0	1.0%PAA	0.2%CMC	[41]
	Y_2O_3	20%	10.0	-	-	[92]
	Y_2O_3	30%	10.0	1.0%PAA	0.3%CMC	[93]
	Y_2O_3:SiO_2	25%	11.0	2.0%PAA	-	[94]
	CeO_2:Yb	-	-	-	-	[95]
Slip casting	Y_2O_3:Al_2O_3	86%	10.0	1.5%PAA	(-)	[96]
	Y_2O_3:Ce	40%	9-11	2.0%PAA	(-)	[97]
	Y_2O_3	30%	10.0	1.5%PMAA	(-)	[98]
	Y_2O_3:Al_2O_3	20%	7-8	0.1%PAA	0.5%PEG	[99]
	Lu_2O_3:Eu	10%	9-10	1%PAA	(-)	[88]
Gelcasting	Y_2O_3	45%	(-)	1.45%PAA	(-)	[100]
Hot pressing	Al_2O_3: (Nd,Eu,Er)	45%	(-)	(-) PMAA	(-)	[101]
Dip coating	$SrAl_2O_4$:Eu^{2+};Dy^{3+}	-	-	3%APTMS	-	[102]
Tape casting	CeO_2:Ga	28%	(-)	0.94% Acidic affine	0.89%PVP	[89]
	$La_{0.9}Sr_{0.1}Ga_{0.8}Mg_{0.8}O_{3-\delta}$ (LSGM)	-	-	1.0% glycerol	-	[103]
	$Ce_{0.9}Gd_{0.1}O_{1.95}$	-	-	-	-	[104]

Ref: reference; vol.%: volume percentage in volume of particles; CMC: Carboxymethylcellulose; PAA: Ammonium polyacrylic acid; PMAA: Ammonium polymethacrylate; PVA: Polyacrylic vinyl alcohol; PEG: Polyethylene Glycol; PVP: Polyvinylpyrrolidone; APTMS: (3-aminopropyl) trimethoxylane; - not reported/used;

Santos *et al.* [43] prepared dysprosium doped yttrium disilicate ($Y_2Si_2O_7$:Dy) suspensions with shear thinning behaviour using 2 wt.% of dispersant and pH of 10 for replica. Fu *et al.* [87] reported that gadolinium doped ceria (CeO_2:Ga) suspensions with 40 vol.% of solids could be stabilized using 5 wt.% of dispersant and pH of 7 for shaping by replica. Dulina *et al.* [88] evaluated the effectiveness of three distinct dispersants, wherein it was found out that the use of 1 wt.%. of Dolapix CE 64 in alkaline pH range was effective to obtain suspensions with low viscosity for gel-casting. Marani *et al.* [89] achieved a suitable rheological condition for tape casting of CeO_2:Ga suspensions by using 0.94% of acidic affine as dispersing agent and 0.89% PVP as plasticizer.

Even though diverse shaping process have been developed and improved, it is evident that many studies need to be performed in colloidal processing of rare earths with the aim to define suitable parameters for shaping. Among shaping processes, bio-prototyping a new designation of replica method [90] is very promising, seeing that it is possible to produce samples with complex shape, including low cost [91].

4.8. Shaping Materials from Suspensions - Replica Method

Replica method proposed by Schwartzwalder [90] consists basically in inserting-taking out a template (in nature or synthetic) in a suspension containing the material that is desired to shape. Considering suspension stability and liquid medium, the solid particles are impregnated in template surface after immersion. The as impregnated template is subjected to the drying process, followed by calcination (to burn out template structure and others aids) and finally by sintering to enhance physical bond between particles and as a consequence, improving mechanical strength of the final material. The main advantage of this process consists in the possibility of using any kind of material dispersed in suspension [105].

Polymeric sponge, carbon sponge, and other synthetic fibres have been used as replica template (Table **6**). Polymeric sponge is still the most used, due to the control of porous size, reproducibility, availability, low price, as well as consolidated knowledge of this material. With rising concern about development of process and components with low environmental impact, there is a great effort to substitute synthetic materials for vegetable structures from biodiversity. In addition, contributions have been presented in order to improve replica process such as, rheological studies on ceramic [105]; double impregnation to enhance thickness of samples [106]; inserting of fibres or aids to enhance mechanical strength [107]; evaluation of thermal de decomposition of replica templates [65].

Our search group has reported approaches on the development of advanced materials by replica method using renewable materials [40-43, 84, 92]. Yttria nettings with homogeneous void shape were produced using wood based netting as template [40]. Biomorphic burners with thermoluminescence response based on dysprosium doped yttrium disilicate were formed from Luffa Cylindrica vegetable sponge [43]. Yttria micro rods with dense micro-

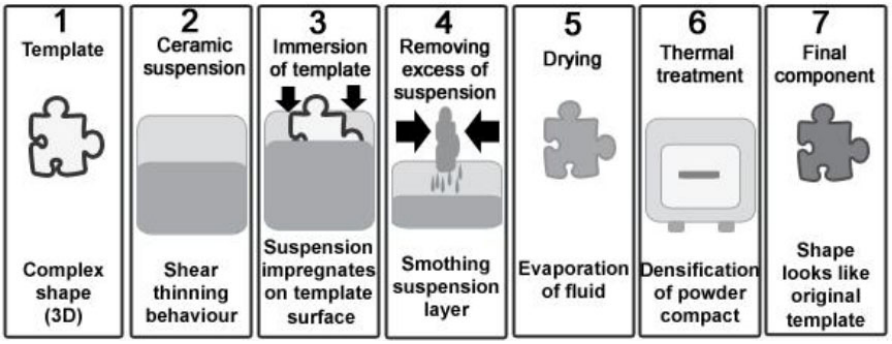

Fig. (14). Representation of replica method from colloidal suspensions.

Table 6. Materials used as template for replica method.

Reference	Template	Suspension
[108]	Polymeric sponge	Al_2O_3
[109]		ZrO_2
[110]		Si_3N_4
[111]		TiO_2
[112]		SiC
[113]	Carbon sponge	ZrO_2
[114]		SiC
[115]		SiO_2
[116]	Wood	TiO_2
[117]		Al_2O_3
[118]		SiC
[119]	Coral	Si_3N_4
[120]		MgO
[121]		Hydroxyapatite
[40]	Cotton	Y_2O_3
[122]		Y_2O_3:TR
[123]		Al_2O_3
[42]	Vegetable sponge	$Y_2Si_2O_7$
[124]		Clay
[43]		$Y_2Si_2O_7$:Dy
[41]		RE_2O_3
[92]	Wheat starch	Y_2O_3:Eu

structure and electron paramagnetic response were shaped from wheat starch templates [92].

4.9. Drying Behavior and Sintering of Green Bodies

Drying behavior of the as shaped bodies addressed as green bodies is a complex step into ceramic processing. The process of removing liquid phase (fluid) comprehends distinct drying phenomenon as, capillary driven flow, viscous deformation, evaporation, and diffusion.

Dimensional heterogeneities, including segregation and cracking are common failures during drying stage [125]. In general, drying behavior consists in three stages as follows: (1) constant rate period (CRP), (2) first falling-rate period (FRP1), and (3) second falling-period (FRP2). At CRP, by capillary-driven transport the fluid is supplied to external surface of the component. At FRP1, evaporation takes place from the fluid meniscus, which turns fluid to retrain into the component body. At FRP2, the remaining fluid is removed from the component body *via* vapour-phase diffusion [53].

To achieve high packing of particles during drying, two aspects have to be considered; dispersion of particles through an effective dispersing method, and control of the compressive flow behavior of particle network applied to drying stress to induce the most suitable consolidation of particles.

The microstructure of the component is a consequence of rheological behavior of suspension, drying behaviour of particle compact and thermal treatment condition of the as shaped body. Thermal treatment aims to enhance physical bond between consolidated particles, which means densification.

Densification model of a powder compact is illustrated in Fig. (**15**) [126]. Firstly, neck growth dominates mass transport between particles by grain boundary diffusion (Fig. **15b**) *i.e*. particle mass diffuses along the grain boundary to the surface to form a neck and as a consequence produces shrinkage (b_1-b_2). The smaller grain donates its mass to the larger one, which reduces the surface to volume ratio. Furthermore, although neck growth ceases the two sintered grains can reduce their free energy if the grain boundary moves through the smaller grain and disappears (b_2- b_3 and b_3-b_4). According to Kellet *et al.* [127], it is achieved *via* coarsening where the energy barrier for grain boundary motion is zero. In the case where the smaller particle is between two larger ones (Fig. **15c**) the same sequential mass transport occurs *i.e*. sintering (c_1-c_2)> grain boundary diffusion (c_2-c_3) > sintering (c_3-c_4). In addition, the two larger grains touch one another (c_3), initiate grain growth and reinitiate shrinkage (c_3-c_4).

Fig. (**16a**) shows optical image of biomorphic dysprosium-yttria sample produced by bio-prototyping [41]. It is seen that the sample is constituted by reticulated architecture like the vegetable template (Fig. **16b**). Sintering

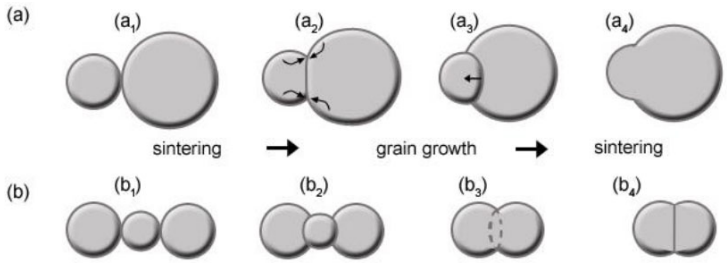

Fig. (15). Densification model of a powder compact by (**a**) two touching particles and (**b**) two larger particles sandwiching a smaller particle.

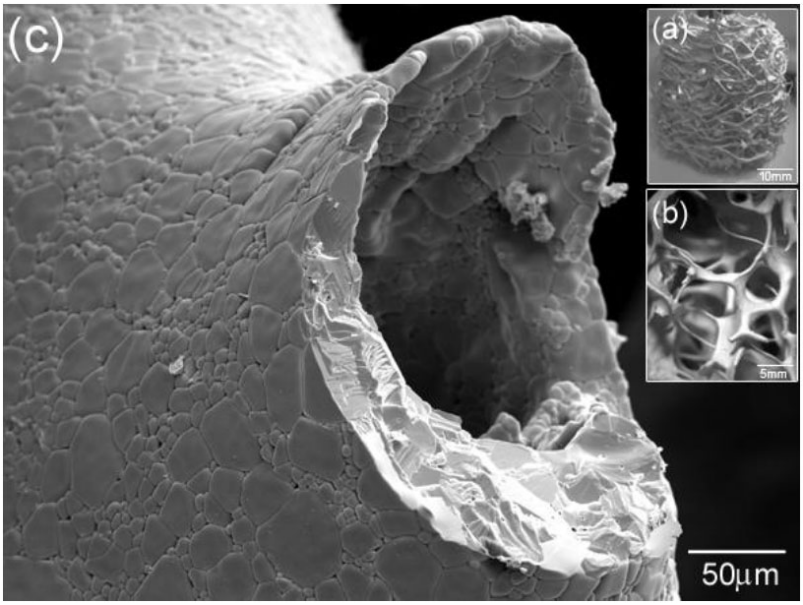

Fig. (16). Development of biomorphic ceramics by bio-prototyping. In (**a**) optical image of dysprosium-yttria sample sintered at 1600°C for 2 h in air; (**b**) ceramic reticulated architecture exhibiting its hollow structure; (**c**) SEM image of a strut showing transgranular fracture and cleavage planes.

at 1600°C for 1h at room atmosphere supplied densification of particles, in which samples presented pycnometric density of 6.03g.cm^{-3}. Besides, surface microstructure of struts constitute of grains with size larger than 5 µm (Fig. **16c**). As fractured struts revealed transgranular fracture and cleavage planes.

CONCLUSION

Colloidal processing is relatively mature, in which excellent reviews have been reported by Hunter *et al.* [1], Moreno [56], Sigmund *et al.* [70], and Lange [128]. Even though rare earths are special group of elements used in highly technological applications, few studies about colloidal processing of these elements have been reported. The purpose of this review goes beyond that most of papers about rare earths have presented. This purpose combines an overview about rare earths with a set of approaches that colloidal processing provides to design, as well as to produce smart materials based on rare earths for diverse applications.

Yttria is still the most used rare earth host for luminescent materials (75%), once it exhibits great chemical and physical similarity with other rare earth elements. Many contributions on the synthesis of yttria nano particles have been reported, but few works about dispersion of concentrated suspensions, shaping and sintering of compact bodies of yttria are found. Moreover, for other rare earth such as europium, erbium, dysprosium, and cerium these studies are rare. Therefore, much information about surface chemistry of these elements is unclear.

Rheology of rare earth suspensions by means of flow curves, including rheological models provides substantial information on ceramic structure. The control of viscosity enables to fit suspension structure for any shaping method, as well as to form compact bodies with near net shape characteristics. Besides, viscosity of fluid is determinant in

diverse subject areas as biology, environmental, food, chemistry, and aerospace. Thus, rheology investigations on rare earths are necessary in order to advance in these fields.

Replica method is a useful procedure to produce ceramic bodies with complex shape by means of coating an organic template with suspension, followed by thermal treatment. With advance of colloidal processing, new shaping process has been proposed as 3D prototyping.

Understanding inter- particle forces of rare earths, how to control them, the use of rheological models as tools to fit suspensions structures for shaping process will advance through new possibilities in related fields such as dosimetry, photonic, bio-prototyping, complex fluids, and general nanotechnology.

CONSENT FOR PUBLICATION

Not applicable.

CONFLICT OF INTEREST

The authors declare no conflict of interest, financial or otherwise.

ACKNOWLEDGEMENTS

We authors are deeply grateful to Dr. Sonia Mello, Dr. Chieko Yamagata, and Dr. Thomaz Restivo from Nuclear and Energy Research Institute (IPEN); MSc. Douglas Will Leite and MSc. William Naville from University Center of FEI. Mr. Pedro Garcia from Almatis Brazil. In addition, we thank to São Paulo Research Foundation (FAPESP, grant #2014/23621-3); National Council for Scientific and Technological Development (CNPq); and Coordination for Improvement of High Degree People (CAPES).

REFERENCES

[1] Hunter, R.J. *Foundations of colloidal science,* Oxford Science: Oxford, **1986**.

[2] Van Gosen, B.S.; Verplanck, P.L.; Long, K.R.; Gambogi, J.; Seal, R.R. *The rare-earth elements-Vital to modern technologies and lifestyles: U.S. Geological Survey Fact Sheet,* U.S. Geological Survey: United States of America, **2014**; p. 4.

[3] Zhanheng, C. Global rare earth resources and scenarios of future rare earth industry. *J. Rare Earths,* **2011**, *29*(1), 1-6.

[4] Gambogi, J. *Mineral Commodity Summaries,* U.S. Geological Survey: 03/31/2017, **2017**.

[5] Schwab, K. The Global Competitiveness Report 2016-2017; World Economic Forum: Switzerland, **2016**; p. 400.

[6] Konings, R.J.; Kovács, A. Thermodynamic properties of the lanthanide(III) halides.*Handbook on the Physics and Chemistry of Rare Earths, K.A.,* **2003**, *Vol. 33*, 147-247.

[7] Wang, X.C.; Zhu, M.G.; Li, W.; Zheng, L.Y.; Zhao, D.L.; Du, X.; Du, A. The Microstructure and magnetic properties of melt-spun CeFeB ribbons with varying Ce content. *Electron. Mater. Lett.,* **2015**, *11*(1), 109-112.

[8] Witas, P.; Goraus, J.; Zajdel, P.; Balin, K.; Koperski, J.; Lelatko, J.; Slebarski, A. Impact of microstructure on the thermoelectric properties of the ternary compound $Ce_3Cu_3Sb_4$. *Mater. Charact.,* **2017**, *123*, 256-263.

[9] Gorni, G.; Cosci, A.; Pelli, S.; Pascual, L.; Duran, A.; Pascual, M.J. Transparent oxyfluoride nano-glass ceramics doped with Pr_3+ and Pr_3+-Yb_3+ for NIR emission. *Front. Mater.,* **2017**, 3.

[10] Jin, Y.; Long, X.Y.; Zhu, Y.N.; Ge, M.Q. Optical performance study of $Sr_2ZnSi_2O_7$:Eu_2+,Dy_3+, $SrAl_2O_4$:EU_2+,Dy_3+ and Y_2O_2S:Eu_3+,Mg_2+,Ti_4+ ternary luminous fiber. *J. Rare Earths,* **2016**, *34*(12), 1206-1212.

[11] Carvalho, E.A.; Freitas, A.M.; Silva, G.H.; Bell, M.J.; Kassab, L.R.; Anjos, V. Thermal and structural analysis of germanate glass and thin films co-doped with silver nanoparticles and rare earth ions with insights from visible and Raman spectroscopy. *Vib. Spectrosc.,* **2016**, *87*, 143-148.

[12] Wu, T.T.; Zhou, J.; Wu, B.L.; Li, W.J. Effect of La_2O_3 content on wear resistance of alumina ceramics. *J. Rare Earths,* **2016**, *34*(3), 288-294.

[13] Zur, L.; Tran, L.T.; Meneghetti, M.; Tran, V.T.; Lukowiak, A.; Chiasera, A.; Zonta, D.; Ferrari, M.; Righini, G.C. Tin-dioxide nanocrystals as Er_3+ luminescence sensitizers: Formation of glass-ceramic thin films and their characterization. *Opt. Mater.,* **2017**, *63*, 95-100.

[14] Jin, F.; Zhang, H.; Wang, W.Z.; Liu, X.; Chen, Q.M. Improvement in structure and superconductivity of $YBa_2Cu_3O_6$+delta ceramics superconductors by optimizing sintering processing. *J. Rare Earths,* **2017**, *35*(1), 85-89.

[15] Pawar, P.P.; Munishwar, S.R.; Gautam, S.; Gedam, R.S. Physical, thermal, structural and optical properties of Dy3+ doped lithium alumino-borate glasses for bright W-LED. *J. Lumin.,* **2017**, *183*, 79-88.

[16] Wang, D.; Ye, Q.; Long, J.; Jin, J.; He, H. Effect of sm on gas-sensing properties of SnO_2 with different oxygen vacancy concentrations. *J. Rare Earths,* **2000**, *18*(1), 30-33.

[17] Muroyama, H.; Asajima, H.; Hano, S.; Matsui, T.; Eguchi, K. Effect of an additive in a CeO_2-based oxide on catalytic soot combustion. *Appl. Catal. A Gen.,* **2015**, *489*, 235-240.

[18] Chen, H.W.; Liu, S.S.; Miao, L.F.; Yu, L.F.; Wang, Y.; Guo, F. Inhibitory effect of lanthanum chloride on migration and invasion of cervical cancer cells. *J. Rare Earths,* **2013**, *31*(1), 94-100.

[19] Kohn, M.J.; Morris, J.; Olin, P. Trace element concentrations in teeth - a modern Idaho baseline with implications for archeometry, forensics, and palaeontology. *J. Archaeol. Sci.,* **2013**, *40*(4), 1689-1699.

[20] U.S. Geological Survey, U. S. G. S., Mineral commodity summaries 2014. Virginia, **2014**; p. 196.

[21] Characteristics of Kyocera Fine Ceramics. Corporation, K., Ed. Kyocera: Japan, **2016**; p. 6.

[22] Hoekstra, H.R.; Gingerich, K.A. High-pressure B-type polymorphs of some rare-earth sesquioxides. *Science,* **1964**, *146*(3648), 1163-1164.

[23] Gourlaouen, V.; Schnedecker, G.; Lejus, A.M.; Boncoeur, M.; Collongues, R. Metastable phases in yttrium-oxide plasma spray deposits and their effect on coating properties. *Mater. Res. Bull.,* **1993**, *28*(5), 415-425.

[24] Navrotsky, A.; Benoist, L.; Lefebvre, H. Direct calorimetric measurement of enthalpies of phase transitions at 2000 degrees-2400 degrees C in yttria and zirconia. *J. Am. Ceram. Soc.,* **2005**, *88*(10), 2942-2944.

[25] Qin, X.; Ju, Y.G.; Bernhard, S.; Yao, N. Flame synthesis of Y_2O_3: Eu nanophosphors using ethanol as precursor solvents. *J. Mater. Res.,* **2005**, *20*(11), 2960-2968.

[26] Govindasamy, A.; Lv, C.; Tsuboi, H.; Koyama, M.; Endou, A.; Kubo, M.; Broclawik, E.; Miyamoto, A. A theoretical study of the effect of Eu ion dopant on the electronic excitations of yttrium oxide and yttrium oxy-sulphide. *Jpn. J. Appl. Phys. 1,* **2006**, *45*(7), 5782-5785.

[27] Xu, Y.N.; Gu, Z.Q.; Ching, W.Y. Electronic, structural, and optical properties of crystalline yttria. *Phys. Rev. B,* **1997**, *56*(23), 14993-15000.

[28] Wang, W.N.; Widiyastuti, W.; Ogi, T.; Lenggoro, I.W.; Okuyama, K. Correlations between crystallite/particle size and photoluminescence properties of submicrometer phosphors. *Chem. Mater.,* **2007**, *19*(7), 1723-1730.

[29] Zhang, H.; Cen, Y.; Chen, L.F.; Zhu, H.Y.; Qian, L.J.; Fan, D.Y. Full-angle collimations of two-dimensional photonic crystals with

ultrahigh-index background materials. *J. Opt-Uk,* **2010**, *12*(4)

[30] Goldburt, E.T.; Kulkarni, B.; Bhargava, R.N.; Taylor, J.; Libera, M. Size dependent efficiency in Tb doped Y_2O_3 nanocrystalline phosphor. *J. Lumin.,* **1997**, *72-74*(0), 190-192.

[31] Wu, Z.K.; Li, N.; Jian, C.; Zhao, W.Q.; Yan, J.Z. Low temperature degradation of Al_2O_3-doped 3Y-TZP sintered at various temperatures. *Ceram. Int.,* **2013**, *39*(6), 7199-7204.

[32] Armani, C.J.; Ruggles-Wrenn, M.B.; Hay, R.S.; Fair, G.E.; Keller, K.A. Creep of polycrystalline yttrium aluminum garnet (YAG) at elevated temperature in air and in steam. *Mat. Sci. Eng. Struct.,* **2014**, *589*, 125-131.

[33] Peng, Q.M.; Zhao, S.S.; Li, H.; Ma, N.; Li, X.J.; Tian, Y.J. High pressure solidification: An effective approach to improve the corrosion properties of Mg-Y based implants. *Int. J. Electrochem. Sci.,* **2012**, *7*(6), 5581-5595.

[34] Lee, K.; Yi, J.E.; Kim, B.; Ko, J.; Jeong, S.; Noh, M.; Lee, S.S. Micro-energy storage system using permanent magnet and high-temperature superconductor. *Sens. Actuators A Phys.,* **2008**, *143*(1), 106-112.

[35] Salhi, R.; Deschanvres, J.L. Efficient upconversion in Er_3+ doped Y_2O_3/Si thin film deposited by aerosol UV-assisted MOCVD process. *J. Lumin.,* **2016**, *170*, 231-239.

[36] Li, S.S.; Ji, Y.H.; Zhang, S.Q.; Zhong, S.L.; Zeng, C.H. Fabrication of Yb_3+/Er_3+ co-doped yttrium-based coordination polymer hierarchical micro/nanostructures: Upconversion luminescence properties and thermal conversion to the corresponding oxides. *CrystEngComm,* **2016**, *18*(36), 6809-6816.

[37] Yavetskiy, R.P.; Baumer, V.N.; Danylenko, M.I.; Doroshenko, A.G.; Ogorodnikov, I.N.; Petrusha, I.A.; Tolmachev, A.V.; Turkevich, V.Z. Transformation-assisted consolidation of Y_2O_3:Eu_3+ nanospheres as a concept to optical nanograined ceramics. *Ceram. Int.,* **2014**, *40*(2), 3561-3569.

[38] Mukherjee, S.; Sudarsan, V.; Sastry, P.U.; Patra, A.K.; Tyagi, A.K. Morphology and luminescence characteristics of combustion synthesized Y_2O_3: (Eu, Dy, Tb) nanoparticles with various amino-acid fuels. *J. Lumin.,* **2014**, *145*, 318-323.

[39] Ikesue, A.; Aung, Y.L. Synthesis of Yb:YAG Ceramics without sintering additives and their performance. *J. Am. Ceram. Soc.,* **2017**, *100*(1), 26-30.

[40] Santos, S.C.; Acchar, W.; Yamagata, C.; Mello-Castanho, S. Yttria nettings by colloidal processing. *J. Eur. Ceram. Soc.,* **2014**, *34*(10), 2509-2517.

[41] Santos, S.C.; Yamagata, C.; Campos, L.L.; Mello-Castanho, S.R. Bio-prototyping and thermoluminescence response of cellular rare earth ceramics. *J. Eur. Ceram. Soc.,* **2016**, *36*(3), 791-796.

[42] Santos, S.C.; Yamagata, C.; Silva, A.C.; Setz, L.F.; Mello-Castanho, S.R. Yttrium disilicate micro-cellular architecture from biotemplating of *Luffa cylindrica. J. Cer. Sci. Technol.,* **2014**, *5*(3), 203-208.

[43] Santos, S.C.; Yamagata, C.; Campos, L.L.; Mello-Castanho, S.R. Processing and thermoluminescent response of porous biomorphic dysprosium doped yttrium disilicate burner. *Mater. Chem. Phys.,* **2016**, *177*, 505-511.

[44] Murray, C.B.; Norris, D.J.; Bawendi, M.G. Synthesis and characterization of nearly monodisperse CdE (E = sulfur, selenium, tellurium) semiconductor nanocrystallites. *J. Am. Chem. Soc.,* **1993**, *115*(19), 8706-8715.

[45] McBain, J.W.; Salmon, C.S. Colloidal electrolytes. soap solutions and their constitution.2. *J. Am. Chem. Soc.,* **1920**, *42*(3), 426-460.

[46] Chang, Y-S.; Chang, Y-H.; Chen, I-G.; Chen, G-J.; Chai, Y-L. Synthesis and characterization of zinc titanate nano-crystal powders by sol-gel technique. *J. Cryst. Growth,* **2002**, *243*(2), 319-326.

[47] Harrison, M.T.; Kershaw, S.V.; Rogach, A.L.; Kornowski, A.; Eychmüller, A.; Weller, H. Wet chemical synthesis of highly luminescent HgTe/CdS core/shell nanocrystals. *Adv. Mater.,* **2000**, *12*(2), 123-125.

[48] Zhai, Y.Q.; Zhao, Q.; Han, Y.; Wang, M.; Yu, J.B. Hydrothermal synthesis, characterization and luminescence properties of orange-red-emitting phosphors SnO_2: Eu. *J. Mater. Sci. Mater. Electron.,* **2016**, *27*(1), 677-684.

[49] Valentini, A.; Carreño, L.V.; Probst, L.F.; Leite, E.R.; Longo, E. Synthesis of Ni nanoparticles in microporous and mesoporous Al and Mg oxides. *Microporous Mesoporous Mater.,* **2004**, *68*(1-3), 151-157.

[50] Dai, Z.R.; Pan, Z.W.; Wang, Z.L. Gallium oxide nanoribbons and nanosheets. *J. Phys. Chem. B,* **2002**, *106*(5), 902-904.

[51] Tscharnuter, W. Photon Correlation Spectroscopy in Particle Sizing.*Encyclopedia of Analytical Chemistry.,* **2000**, , 5549-5485.

[52] (a) Jaycock, M.J.; Parfitt, G.D. *Chemistry of Interfaces.,* **1981**, (b) Parfitt, G.D.; Sing, K.S. *Characterization of Powders Surfaces.,* **1976**, (c) Vold, R.D.; Vold, M.J. *Colloid and Interface Chemistry.,* **1983**, (d) Reed, J. *Principles of Ceramics Processing.,* 2nd ed.; John Wiley & Sons: New York, 1995; Vol. 1.

[53] Lewis, J.A. Colloidal processing of ceramics. *J. Am. Ceram. Soc.,* **2000**, *83*(10), 2341-2359.

[54] Derjaguin, B.V.; Churaev, N.V.; Muller, V.M. The Derjaguin—Landau—Verwey—Overbeek (DLVO) Theory of Stability of Lyophobic Colloids. In Surface Forces, Springer US: **1987**; pp. 293-310.

[55] Shaw, D.J. *Introduction to Colloid and Surface Chemistry.,* (4th ed.) 4th ed. **1989**, , 306.

[56] Moreno, R. *Reología de suspensiones cerámicas.,* Consejo Superior de Investigaciones Científicas: Madrid, **2005**.

[57] Hunter, R.J. *Zeta potential in colloid science.,* Academic Press: Londres, **1981**.

[58] Suphantharida, P.; Osseo-Asare, K. Cerium oxide slurries in CMP. Electrophoretic mobility and adsorption investigations of ceria/silicate interaction. *J. Electrochem. Soc.,* **2004**, *151*(10), G658-G662.

[59] Ozawa, M.; Hattori, M. Ultrasonic vibration potential and point of zero charge of some rare earth oxides in water. *J. Alloys Compd.,* **2006**, *408*, 560-562.

[60] Subramanian, S.; Chattha, M.S.; Peters, C.R. Characterization of Lanthana alumina composite oxides. *J. Mol. Catal.,* **1991**, *69*(2), 235-245.

[61] Nechaev, E.A. Adsorption of methylene-blue on oxides from aqueous-solutions. *Colloid J. USSR,* **1980**, *42*(2), 311-314.

[62] Nechayev, Y.A.; Sheyin, V.N. Ions specific absorption on oxides. *Коллоид. ж.,* **1979**, 41.

[63] Ahmed, S.M. Studies of the double layer at oxide-solution interface. *J. Phys. Chem.,* **1969**, *73*(11), 3546-3555.

[64] Wei, W.C.; Wang, S.C.; Ho, F.Y. Electrokinetic properties of colloidal zirconia powders in aqueous suspension. *J. Am. Ceram. Soc.,* **1999**, *82*(12), 3385-3392.

[65] Santos, S.C. *Processamento coloidal de componentes cerâmicos para queimadores de gás. Dissertação de Mestrado, Universidade de São Paulo.,* **2010**,

[66] Oosawa, F.; Asakura, S. Surface Tension of high-polymer solutions. *J. Chem. Phys.,* **1954**, *22*(7), 1255-1255.

[67] Vincent, B.; Luckham, P.F.; Waite, F.A. Effect of free polymer on the stability of sterically stabilized dispersions. *J. Coll. Interf. Sci.,* **1980**, *73*(2), 508-521.

[68] Ryszard Sprycha, J.J. Egon Matijevic, zeta potential and surface charge of monodispersed colloidal Yttrium (III) oxide and basic carbonate. *J. Coll. Interf. Sci.,* **1991**, *149*, 562-568.

[69] *Manual of symbols and terminology for physicochemical quantities and units.,* **1979**, *Vol. 2*

[70] Sigmund, W.M.; Bell, N.S.; Bergstrom, L. Novel powder-processing methods for advanced ceramics. *J. Am. Ceram. Soc.,* **2000**, *83*(7), 1557-1574.

[71] Schramm, G. *A practical approach to rheology and rheometry.,* Gebrueder HAAKE GmbH: Alemanha, **1994**.

[72] Santos, S.C. *Desenvolvimento de queimadores para iluminação a gás à base de silicato de terras raras.,* **2014**,

[73] Combe, E.; Guilmeau, E.; Savary, E.; Marinel, S.; Cloots, R.; Funahashi, R.; Boschini, F. Microwave sintering of Ge-doped In_2O_3 thermoelectric ceramics prepared by slip casting process. *J. Eur. Ceram. Soc.,* **2015**, *35*(1), 145-151.

[74] Lin, H.; Tang, F.; Chen, W.; Guo, W.; Huang, Q.; Wang, N.; Guan, L.; Cao, Y.; Zhang, G. Diode-pumped tape casting planar waveguide YAG/Nd:YAG/YAG ceramic laser. *Opt. Express,* **2015**, *23*(6), 8104-8112.

[75] Lange, F.F.; Miller, K.T. Pressure filtration - consolidation kinetics and mechanics. *Am. Ceram. Soc. Bull.,* **1987**, *66*(10), 1498-1504.

[76] Miller, K.T.; Melant, R.M.; Zukoski, C.F. Comparison of the compressive yield response of aggregated suspensions: Pressure filtration, centrifugation, and osmotic consolidation. *J. Am. Ceram. Soc.,* **1996**, *79*(10), 2545-2556.

[77] Singh, R.; Chhabra, M. Three-Dimensional Printing.*Reference Module in Materials Science and Materials Engineering.,* **2017**,

[78] Maleksaeedi, S.; Paydar, M.H.; Ma, J. Centrifugal gel casting: A combined process for the consolidation of homogenous and reliable ceramics. *J. Am. Ceram. Soc.,* **2010**, *93*(2), 413-419.

[79] Wang, J.; Edirisinghe, M.J. Ceramic Injection Molding.*Reference Module in Materials Science and Materials Engineering.,* **2016**,

[80] Pollinger, J.P.; Khalfalla, Y.E.; Benyounis, K.Y. Gel Casting.*Reference Module in Materials Science and Materials Engineering.,* **2016**,

[81] Gauckler, L.J.; Graule, T.; Baader, F. Ceramic forming using enzyme catalyzed reactions. *Mater. Chem. Phys.,* **1999**, *61*(1), 78-102.

[82] Freitas, C.; Vitorino, N.; Ribeiro, M.J.; Abrantes, J.C.; Frade, J.R. Extrusion of ceramic emulsions: Preparation and characterization of cellular ceramics. *Appl. Clay Sci.,* **2015**, *109*, 15-21.

[83] Soderznik, M.; Korent, M.; Soderznik, K.Z.; Katter, M.; Ustuner, K.; Kobe, S. High-coercivity Nd-Fe-B magnets obtained with the electrophoretic deposition of submicron TbF_3 followed by the grain-boundary diffusion process. *Acta Mater.,* **2016**, *115*, 278-284.

[84] Santos, S.C.; Yamagata, C.; Acchar, W.; Castanho, S.R. Yttria nettings by replica processing. *Mater. Sci. Forum,* **2014**, *798*, 3.

[85] Peng, W.J.; Wu, G.X.; Peng, H.; Ding, D.J.; Yu, Y.W.; Zhang, J.Y. The effect of Al-5 wt%Ti-0.2 wt%B on the solidification characteristics of 55 wt%Al-Zn-1.6 wt%Si alloy in hot-dip coating. *Surf. Coat. Tech.,* **2016**, *306*, 378-389.

[86] Lopez, R.; Zarate, J.; Aguilar, E.A.; Munoz-Saldana, J. Preparation of neodymium-doped yttrium aluminum garnet powders and fibers. *J. Rare Earths,* **2008**, *26*(5), 670-673.

[87] Fu, Y-P.; Liu, Y-C.; Hu, S-H. Aqueous tape casting and crystallization behavior of gadolinium-doped ceria. *Ceram. Int.,* **2009**, *35*(8), 3153-3159.

[88] Dulina, N.A.; Deineka, T.G.; Yavetskiy, R.P.; Sergienko, Z.P.; Doroshenko, A.G.; Mateychenko, P.V.; Vovk, O.M.; Matveevskaya, N.A. Comparison of dispersants performance on the suspension Lu_2O_3:Eu_3+ stability and high-density compacts on their basis. *Ceram. Int.,* **2011**, *37*(5), 1645-1651.

[89] Marani, D.; Sudireddy, B.R.; Bentzen, J.J.; Jorgensen, P.S.; Kiebach, R. Colloidal stabilization of cerium-gadolinium oxide (CGO) suspensions *via* rheology. *J. Eur. Ceram. Soc.,* **2015**, *35*(10), 2823-2832.

[90] Schwartzwalder, K.; Somers, A.V. Method of Making Porous Ceramic. U.S. Patent 3,090,094, **1963**.

[91] Studart, A.R.; Gonzenbach, U.T.; Tervoort, E.; Gauckler, L.J. Processing routes to macroporous ceramics: A review. *J. Am. Ceram. Soc.,* **2006**, *89*(6), 1771-1789.

[92] Santos, S.C.; Rodrigues, J.; Campos, L.L. Radiation effects on microstructure and EPR signal of yttrium oxide rods. *IOP Conf. Ser.: Mater. Sci. Eng.,* **2017**, *169*(1), 012009.

[93] Santos, S.C.; Yamagata, C.; Campos, L.L.; Mello-Castanho, S.R. Processing, microstructure and thermoluminescence response of biomorphic yttrium oxide ceramics. *Ceram. Int.,* **2016**, *42*(11), 13291-13295.

[94] Santos, S.C.; Acchar, W.; Silva, A.C.; Yamagata, C.; Mello-Castanho, S.R. Yttrium disilicate stability in aqueous medium. In 57◦ Congresso Brasileiro de Cerâmica e 5◦ Congresso Ibero Americano de Cerâmica, Hotel Praiamar, Natal, Rio Grande do Norte, RN, Brasil, **2013**.

[95] Qiu, K.; Hayden, A.C. Premixed gas combustion stabilized in fiber felt and its application to a novel radiant burner. *Fuel,* **2006**, *85*(7-8), 1094-1100.

[96] Li, X.; Li, Q. YAG ceramic processed by slip casting *via* aqueous slurries. *Ceram. Int.,* **2008**, *34*(2), 397-401.

[97] Sonoda, K.; Higashi, K.; Ono, H.; Sameshima, S.; Hirata, Y. Surface properties and aqueous processing of rare earth-doped ceria powders by coprecipitation method. *Novel Synth. Process. Ceram.,* **1999**, *159*(1), 169-174.

[98] Jin, L.L.; Mao, X.J.; Wang, S.W.; Dong, M.J. Optimization of the rheological properties of yttria suspensions. *Ceram. Int.,* **2009**, *35*(2), 925-927.

[99] Appiagyei, K.A.; Messing, G.L.; Dumm, J.Q. Aqueous slip casting of transparent yttrium aluminum garnet (YAG) ceramics. *Ceram. Int.,* **2008**, *34*(5), 1309-1313.

[100] Takai, C.; Tsukamoto, M.; Fuji, M.; Takahashi, M. Control of high solid content yttria slurry with low viscosity for gelcasting. *J. Alloys Compd.,* **2006**, *408*, 533-537.

[101] Bodisova, K.; Klement, R.; Galusek, D.; Pouchly, V.; Drdlik, D.; Maca, K. Luminescent rare-earth-doped transparent alumina ceramics. *J. Eur. Ceram. Soc.,* **2016**, *36*(12), 2975-2980.

[102] Li, J.; Zhao, Y.; Ge, M.Q.; Fu, S.D.; Lin, T. Superhydrophobic and luminescent cotton fabrics prepared by dip-coating of APTMS modified $SrAl_2O_4$:Eu_2+,Dy_3+ particles in the presence of SU8 and fluorinated alkyl silane. *J. Rare Earths,* **2016**, *34*(7), 653-660.

[103] Zhang, N.Q.; Sun, K.N.; Zhou, D.R.; Jia, D.C. Study on properties of LSGM electrolyte made by tape casting method and applications in SOFC. *J. Rare Earths,* **2006**, *24*, 90-92.

[104] Cheng, J.G.; Zha, S.W.; Huang, J.; Liu, X.Q.; Meng, G.Y. Sintering behavior and electrical conductivity of Ce0.9Gd0.1O1.95 powder prepared by the gel-casting process. *Mater. Chem. Phys.,* **2003**, *78*(3), 791-795.

[105] Luyten, J.; Mullens, S.; Cooymans, J.; De Wilde, A.M.; Thijs, I.; Kemps, R. Different methods to synthesize ceramic foams. *J. Eur. Ceram. Soc.,* **2009**, *29*(5), 829-832.

[106] Yao, X.M.; Tan, S.H.; Huang, Z.R.; Jiang, D.L. Effect of recoating slurry viscosity on the properties of reticulated porous silicon carbide ceramics. *Ceram. Int.,* **2006**, *32*(2), 137-142.

[107] Pu, X.P.; Liu, X.J.; Qiu, F.G.; Huang, L.P. Novel method to optimize the structure of reticulated porous ceramics. *J. Am. Ceram. Soc.,* **2004**, *87*(7), 1392-1394.

[108] Saggiowoyansky, J.; Scott, C.E.; Minnear, W.P. Processing of porous ceramics. *Am. Ceram. Soc. Bull.,* **1992**, *71*(11), 1674-1682.

[109] Sharifi, H.; Divandari, M.; Khavandi, A.; Idris, M.H. Effect of Al powder and silica sol on the structure and mechanical properties of Al_2O_3-ZrO_2 foams. *Acta Metall. Sin-Engl.,* **2010**, *23*(4), 241-247.

[110] Pan, J.M.; Yan, X.H.; Cheng, X.N.; Lu, Q.B.; Wang, M.S.; Zhang, C.H. Preparation of SiC nanowires-filled cellular SiCO ceramics from polymeric precursor. *Ceram. Int.,* **2012**, *38*(8), 6823-6829.

[111] Lee, J.H.; Kim, H.E.; Shin, K.H.; Koh, Y.H. Improving the strength and biocompatibility of porous titanium scaffolds by creating elongated pores coated with a bioactive, nanoporous TiO_2 layer. *Mater. Lett.,* **2010**, *64*(22), 2526-2529.

[112] Yao, X.M.; Tan, S.H.; Zhang, X.Y.; Huang, Z.R.; Jiang, D.L. Low-temperature sintering of SiC reticulated porous ceramics with MgO-Al_2O_3-SiO_2 additives as sintering aids. *J. Mater. Sci.,* **2007**, *42*(13), 4960-4966.

[113] Zhang, H.; Li, H.; Li, W.; Meng, S.; Li, D. Preparation of TiO_2, CeO_2, and ZrO_2 hierarchical structures in "one-pot" reactions. *J. Colloid Interface Sci.,* **2009**, *333*(2), 764-770.

[114] Jung, I.C.; Kwon, Y.D.; Lee, J.; Min, B.K. Synthesis of B4C nanobelts in porous SiC bodies. *J. Nanosci. Nanotechnol.,* **2011**, *11*(7), 6555-6558.

[115] Yang, Y.; Shi, E.; Li, P.; Wu, D.; Wu, S.; Shang, Y.; Xu, W.; Cao, A.; Yuan, Q. A compressible mesoporous SiO_2 sponge supported by a carbon nanotube network. *Nanoscale,* **2014**, *6*(7), 3585-3592.

[116] Liu, Z.T.; Fan, T.X.; Zhang, W.; Zhang, D. The synthesis of hierarchical porous iron oxide with wood templates. *Microporous Mesoporous Mater.,* **2005**, *85*(1-2), 82-88.

[117] Tang, S.K.; Cui, X.L.; Gu, L.; Zhou, H.; Zhang, X.W. A novel co-templating method for hierarchical mesoporous alumina monoliths replica. *Funct. Mater. Lett. (Singap.),* **2013**, *6*(6)

[118] Sieber, H.; Hoffmann, C.; Kaindl, A.; Greil, P. Biomorphic cellular ceramics. *Adv. Eng. Mater.,* **2000**, *2*(3), 105-109.

[119] Rambo, C.R.; Sieber, H.; Genova, L.A. Synthesis of porous biomorphic alpha/beta-Si_3N_4 composite from sea sponge. *J. Porous Mater.,* **2008**, *15*(4), 419-425.

[120] Niu, H.X.; Yang, Q.; Tang, K.B.; Yie, Y. Self-assembly of porous

MgO nanoparticles into coral-like microcrystals. *Scr. Mater.,* **2006**, *54*(10), 1791-1796.

[121] Roy, D.M.; Linnehan, S.K. Hydroxyapatite formed from coral skeletal carbonate by hydrothermal exchange. *Nature,* **1974**, *247*(5438), 220-222.

[122] Santos, S.C.; Yamagata, C.; Mello-Castanho, S.R.H. Perspectives on the development of porous burners in Brazil. *J. Mater. Sci. Appl.,* **2014**.

[123] Fan, T.X.; Sun, B.H.; Gu, J.J.; Zhang, D.; Lau, L.W. Biomorphic Al_2O_3 fibers synthesized using cotton as bio-templates. *Scr. Mater.,* **2005**, *53*(8), 893-897.

[124] Silva, S.A.; Brunelli, D.D.; Melo, F.C.; Thim, G.P. Preparation of a reticulated ceramic using vegetal sponge as templating. *Ceram. Int.,* **2009**, *35*(4), 1575-1579.

[125] Chiu, R.C.; Cima, M.J. Drying of granular ceramic films.2. Drying stress and saturation uniformity. *J. Am. Ceram. Soc.,* **1993**, *76*(11), 2769-2777.

[126] Lange, F.F.; Kellett, B.J. Thermodynamics of densification: II, grain growth in porous compacts and relation to densification. *J. Am. Ceram. Soc.,* **1989**, *72*(5), 735-741.

[127] Kellett, B.J.; Lange, F.F. Thermodynamics of densification: I, sintering of simple particle arrays, equilibrium configurations, pore stability, and shrinkage. *J. Am. Ceram. Soc.,* **1989**, *72*(5), 725-734.

[128] Lange, F.F. Colloidal processing of powder for reliable ceramics. *Curr. Opin. Solid. St. M,* **1998**, *3*(5), 496-500.